

# Three-Dimensional Specific Patterns Based on the Keller-Segel Model

Hiroto Shoji<sup>1,2\*</sup> Makiko Nonomura<sup>2,3</sup> and Kohtaro Yamada<sup>4</sup>

<sup>1</sup>Department of Physics, Graduate School of Medicine, Kyoto Prefectural University of Medicine, Kyoto 603-8334, Japan

<sup>2</sup>PRESTO, Japan Science and Technology Agency, 4-1-8 Honcho, Kawaguchi, Saitama 332-0012, Japan

<sup>3</sup>Department of Mathematical Information Engineering, College of Industrial Technology, Nihon University, 1-2-1 Izumi-cho, Narashino, Chiba 275-8575, Japan

<sup>4</sup>Liberal Arts Division, Anan National College of Technology, 265 Aoki Minobayashi, Anan, Tokushima 774-0017, Japan

\*E-mail address: shoji@koto.kpu-m.ac.jp

(Received November 1, 2011; Accepted March 11, 2012)

Aggregation patterns in the volume-filling Keller-Segel model are studied numerically. Three-dimensional specific patterns, such as P-surface, perforated lamellar, are appeared. These patterns never exist in lower dimensions. The relative stability analysis of these patterns is also performed numerically on the basis of the derived free energy and of the robustness against perturbation.

**Key words:** Chemotaxis, Keller-Segel Model, Pattern Selection, Stability Analysis

## 1. Introduction

A large number of insects and animals rely on their acute senses of smell for conveying information between members of the species. These chemotactic behavior (e.g. the movement following the gradient of chemicals) were mathematically modeled by Keller and Segel (1970), which is now called the Keller-Segel (KS) model. For four decades, KS models have been studied numerically and analytically (Murray, 1993; Horstmann, 2003). One question concerns the form of the blow-up and the problem of continuation after blow-up (Nagai, 1995). Another aspect relates to the variety of functional forms for the chemotactic sensitivity (Hillen and Painter, 2001; Horstmann, 2003). However, almost all of the previous investigations are restricted to one or two dimensions, where only stripes and spots are concerned.

In this letter, we study aggregation patterns in a three-dimensional (3D) KS model. Hillen and Painter (2009) demonstrated transient spherical patterns, and they carried out numerical stability analysis in three dimensions. However, apart from simple extensions of two-dimensional cases such as spherical, cylinders, and lamellar patterns, there should be essential new patterns in three dimensions.

## 2. Volume-Filling KS Model

The model which we shall explore is the following the volume-filling Keller-Segel model (Hillen and Painter, 2001)

$$\frac{\partial u}{\partial t} = \nabla \cdot [D_u \nabla u - \beta u (1 - u) \nabla c], \quad (1)$$

$$\frac{\partial c}{\partial t} = D_c \nabla^2 c + \lambda u - k^2 c, \quad (2)$$

where  $\beta$ ,  $k$ ,  $D_u$ , and  $D_c$  are all positive.  $u(\vec{r}, t)$  and  $c(\vec{r}, t)$  describe the densities of bacteria and the secreted chemical, respectively. The density(population)-sensing term in which the chemotactic response is switched off at high cell densities by parabolic function. This system is now called the volume-filling KS model (Hillen and Painter, 2001). The global existence of its asymptotic solutions was shown by Hillen and Painter (2001). The volume-filling idea was applied to biological phenomena. Dolak and Hillen (2003) constructed a mathematical model for the pattern formation of *Dictyostelium discoideum* and *Salmonella typhimurium*.

Equations (1) and (2) have only one time-independent uniform solution given by  $(\bar{u}, \bar{c}) = (u_0, \lambda_0 u_0 / k^2)$ . The linear stability analysis of this solution can be readily carried out. We introduce the small deviation from the solution  $(\delta u, \delta c) \sim \exp(\gamma t + i\vec{q} \cdot \vec{r})$ . Substituting  $(u, c) = (\bar{u} + \delta u, \bar{c} + \delta c)$  into Eqs. (1) and (2), we obtain the eigenvalue  $\gamma$  as a function of the wavenumber  $q$ . It is found that the uniform solution becomes unstable, i.e.  $\gamma$  is positive, when  $\{D_u k^2 - \lambda \beta \bar{u} (1 - \bar{u})\} / D_u D_c > 0$  is satisfied.

We have carried out numerical simulations for coupled set of Eqs. (1) and (2) in three dimensions. The space is divided into  $N^3$  cubic cells that the length of an edge is  $\delta x$ . In this situation, the size of space is given by  $L = \delta x \cdot N$ . The periodic boundary conditions are imposed at boundaries of cubes. The forward Euler integration method augmented by upwind scheme to calculate the chemotactic components is used with time step  $\delta t = 0.0005$ .

Numerical calculation of chemotaxis systems requires close attention when the validity of numerical simulations is considered (Hillen and Painter, 2001). Simulations have been checked with a variety of time discretizations, and verified that the obtained patterns shown below are almost independent of the time step. If the system size is large, it takes too much time to obtain asymptotic patterns. Therefore, we selected  $N = 32$ . Moreover, the forward Euler integration method with the center difference finite scheme

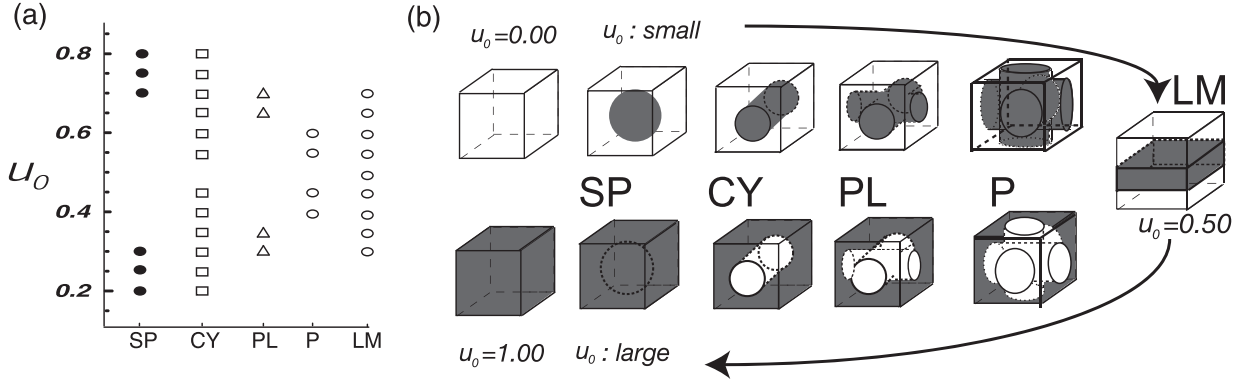


Fig. 1. (a) Five stationary solutions for  $D_u = 1.0$ ,  $D_c = 50.0$ ,  $\beta = 10.0$ ,  $k^2 = 50.0$ , and  $\lambda = 40.0$ . The explanations of SP, CY, PL, P and LM are provided in the text. (b) Schematically showing the obtained patterns SP, CY, PL, P and LM.

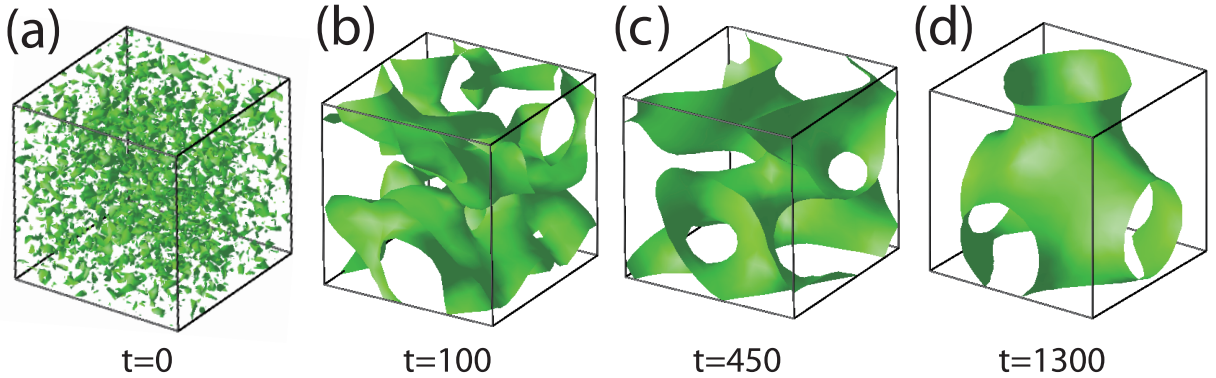


Fig. 2. Time evolution of P-surface for  $u_0 = 0.45$  and  $L = \delta x N$  with  $\delta x = 0.70$  and  $N = 32$ . The other parameters are same as in Fig. 1. In order to make the initial randomness visible, the domain in (a) represents the isosurface of  $u = 0.45060$ , whereas those in (b)–(d) represent the isosurfaces of  $u = 0.45$ .

to discretize the spatial derivatives was also applied.

We start with the uniform solution  $(u, c) = (u_0, \lambda u_0/k^2)$  in an unstable condition with a small superimposed random perturbation. As the global existence of solution in Eqs. (1) and (2) was shown analytically (Hillen and Painter, 2001), the distributions continuously evolve without blow up of distributions, leading to the gradual aggregation of cell density of  $u$ .

The asymptotic stationary solutions obtained numerically are summarized in Fig. 1, where a lot of random initial conditions and  $\delta x$  were given for a given value of  $u_0$ . It should be noted that this set of simulations is very systematic and detailed. For example, we performed simulations for  $u_0 = 0.30$  starting from 5 different random initial conditions and for  $200 = 5 \times 40$  values of  $L = \delta x N$ . This implies that there are independent runs for only one value of  $u_0$ .

It is found that three or four different patterns are obtained for in Fig. 1(a). The abbreviations LM, CY, and SP mean lamellar, cylinder, and sphere, respectively. The remaining P and PL are explained below.

The formation of P for  $u_0 = 0.45$  is displayed in Fig. 2. Figures 3(a) and (b) shows the obtained patterns translated the mass of center of the patten to the center of cubic, and viewed in different two directions. Figure 3(c) shows the stationary profiles of  $u$  and  $c$  measured along the red arrow shown in Figs. 3(a) and (b). It should be noted that

the distributions have sharp interfaces separating between two domains. This pattern is composed of surfaces made of six cylinders as shown in Figs. 2(d) and 3. This pattern is called Schwarz' primitive surface (P-surface), which was first described by Hermann A. Schwarz (1890). The interest in this surface in those days was due to the experimental observation that bi-layers of lipids or surfactants in water solutions form at suitable thermodynamic conditions ordered bi-continuous structures (Luzzati and Spegel, 1867). In the case of  $u_0 = 0.55$ , the distributions are upside down. The P-surface is known as one of the minimal surfaces with the average curvature equal to zero everywhere. This pattern is a new one found in the full 3D computation in nonequilibrium systems.

The asymptotic pattern PL for  $u_0 = 0.35$  is shown in Fig. 4. This pattern is composed of surfaces intersected with four cylinders. When PL connected periodically, the patterns are composed by the lamellar with holes. Therefore, we called PL as perforated lamellae. The inside of perforated lamellae has high density, whereas the remaining space has low density. In the case of  $u_0 = 0.65$ , the distributions are upside down.

### 3. Stability Analysis of Obtained Patterns

As mentioned above, some patterns can be obtained for same  $u_0$ . One of the basic problems is to determine the most stable structure. However, this is highly nontrivial be-

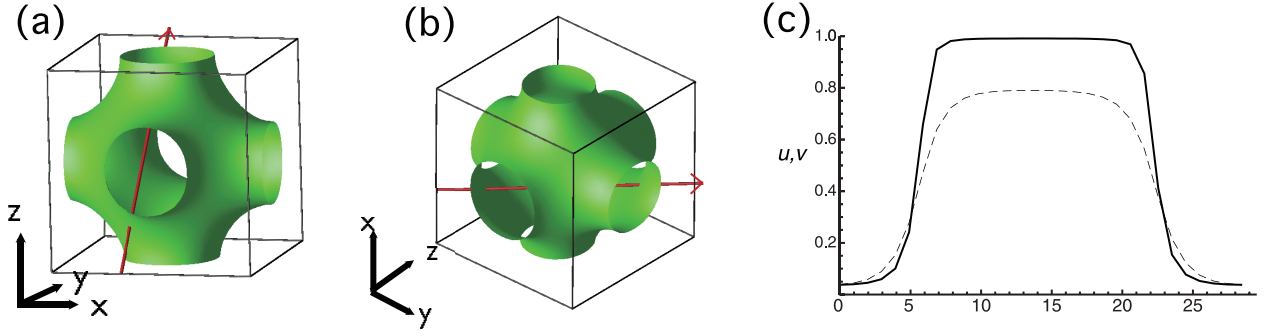


Fig. 3. (a), (b) Isosurface of P surface obtained by Eqs. (1) and (2) for  $u_0 = 0.45$  from different view directions. (c) Spatial variations of concentrations  $u$  (solid line) and  $c$  (dotted line) along the red arrow in (a) and (b).

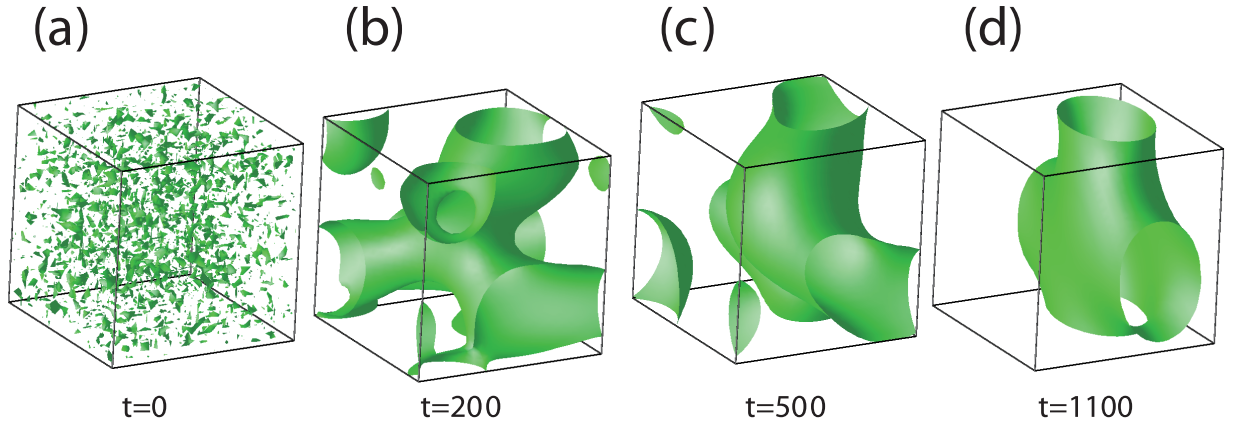


Fig. 4. Time evolution of perforated lamellae for  $u_0 = 0.35$ , and  $L = \delta x N$  with  $\delta x = 0.63$  and  $N = 0.32$ . The other parameters are same as in Fig. 1. In order to make the initial randomness visible, the domains in (a) represent the isosurface of  $u = 0.35075$ , whereas those in (b)–(d) represent the isosurface of  $u = 0.35$ .

cause Eqs. (1) and (2) are nonvariational with no Lyapunov functional. Here, we employ two methods to examine the stability as follows.

One of the methods is to derive approximately a Lyapunov functional for Eqs. (1) and (2) (Chavanis, 2003). In the limit  $D_c \rightarrow +\infty$ , one may set  $\partial c / \partial t = 0$  in Eq. (2), so that Eq. (1) can be viewed as a nonlinear mean-field Fokker-Planck equation associated with a Langevin dynamics of the form

$$\frac{d\vec{r}}{dt} = (1 - u)\nabla c + \sqrt{2D_u}\vec{R}(t), \quad (3)$$

where  $\vec{R}(t)$  is white noise. Equation (3) describes a point organism  $\vec{r}$  performing a random walk biased in the direction of a drift velocity proportional to the local density of  $u$  and to the local gradient of  $c$ . In this situation, the physical temperature  $T = \beta D_u$  defined by the Einstein relation is fixed instead of the energy since  $D_u \propto T$  (Chavanis, 2003).

Here, we can consider the Helmholtz free energy as a Lyapunov functional,

$$F = -\frac{1}{2} \int u c d\vec{r} + T \int \{u \ln u + (1 - u) \ln(1 - u)\} d\vec{r}, \quad (4)$$

where the first term represents the self-interaction and the second term expresses the entropy. Chavanis (2003) used

the entropy of Fermi-Dirac type, because the density always remains bounded by parabolic terms in Eq. (1) as shown in Fig. 3(c). In Chavanis (2003), it was shown  $\dot{F} \leq 0$ , which is similar to the proper version of the H-theorem of the canonical ensemble.

We evaluate the Helmholtz free energy of SP, CY, PL, P, LM and uniform distributions by substituting the asymptotic values of  $u$  and  $c$  directly into Eq. (4). These asymptotic values were prepared as follows.

For each parameter  $u_0$  and  $\lambda$ , the distribution of  $u$  is estimated as  $u(\vec{r}) = 1/(1 + e^{B\vec{r}+A})$  corresponding to  $\dot{F} = 0$  (Chavanis, 2003). For example, in the case of the SP, numerical calculations are started from the distributions such as

$$u(\vec{r}) = \frac{1}{1 + \exp \left[ B \sqrt{(x - x_0)^2 + (y - y_0)^2 + (z - z_0)^2} \right]}, \quad (5)$$

where  $(x_0, y_0, z_0)$  is its center.  $B$  is the slope of the interface between cell and non-cell areas. The distribution of  $c(\vec{r})$  can be expressed numerically by the solution of Helmholtz equation using Bessel functions. Carrying out the numerical simulation, in which these distributions are employed as initial conditions, for a sufficient long time such that the distributions would no longer change, we can obtain the equilibrium distributions. Introducing the each pattern (SP,

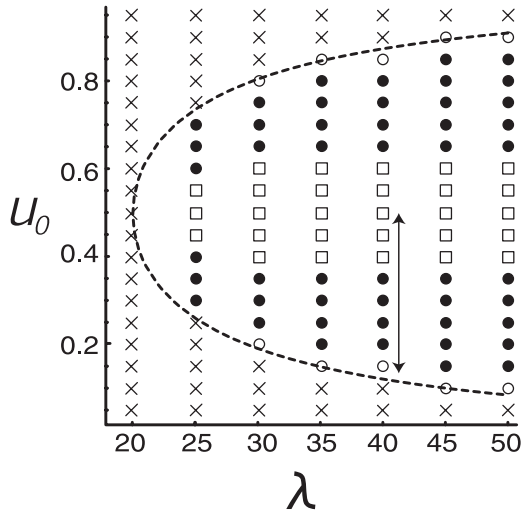


Fig. 5. Phase diagram in the  $u_0 - \lambda$  plane for  $D_u = 1.0$ ,  $D_c = 50.0$ ,  $\beta = 10.0$  and  $k^2 = 50.0$ . The most stable regions for LM, CY, and SP patterns obtained by the stability analysis based on the derived free energy are indicated by  $\square$ ,  $\bullet$ , and  $\circ$ , respectively.  $\times$  represents the region where uniform patterns are the most stable. The dotted curve represents the condition for the linear stability analysis. The arrow indicates the parameter area where the stability analysis is performed on the basis of the robustness against perturbation.

Table 1. Maximum perturbation strength beyond which the original structure does not survive at  $u_0 = 0.30$ .

Patterns	Strength
Cylinder (CY)	1.15
Lamellar (LM)	1.05
Sphere (SP)	1.03
Perforated Lamellar (PL)	0.85

CY, PL, P, LM, and uniform patterns) into Eq. (4), we compare the values of the free energy for each pattern. We obtain the smallest value of the free energy among SP, CY, PL, P, LM patterns or uniform distributions. Then, we determine the patterns with smallest values as the most stable ones.

On repeating the numerical simulations for different values of  $\delta x$  we found that  $F$  is a monotonic decreasing function with respect to the system size  $\delta x$  for each pattern. Therefore, we compared the values of the free energy for each pattern for the system size  $L = 22.4$ . Then, we obtained the smallest value of the Lyapunov functional among SP, CY, LM, and PL patterns or uniform distributions. By repeating the numerical simulations for each value of  $u_0$  and  $\lambda$  we obtained the result shown in Fig. 5 for  $D_u = 1.0$ ,  $D_c = 50.0$ ,  $\beta = 10.0$ ,  $k^2 = 50.0$ . We found that the obtained patterns shown in Fig. 1 are similar to the patterns with the smallest values of the free energy shown in Fig. 5, and PL and P patterns are ones with the smallest values of the free energy in no area.

The other is to explore numerically the volume of the basin of each stable pattern. To this end, we have carried out the following simulations. We provide the patterns of SP, CY, PL, P, and LM for a given value of  $u_0$  as initial con-

ditions and start numerical simulations for Eqs. (1) and (2) with a certain amplitude of random force and continue numerical simulations up to  $4 \times 10^5$  time steps. Then, we turn off the random forces and continue numerical simulations up to the same steps as the above and see whether the initial structure appears or not. In this way, we can obtain numerically the upper limit of the noise amplitude below which the initial structure recovers. Table 1 shows the result for  $u_0 = 0.30$  that CY has the widest basin of attractor in the functional space. If the amplitude of noise is larger than 1.15, CY is broken and one of the other structures LM, SP or PL appears asymptotically.

Similarly, we have carried out numerical simulation among  $0.15 \leq u_0 \leq 0.50$  for  $D_u = 1.0$ ,  $D_c = 50.0$  and system size  $L = 22.4$  in Eqs. (1) and (2), which are same conditions indicated by the arrow in Fig. 5. We obtained the identical information about the stability, that is, SP has the widest basin of attractor at  $u_0 = 0.15$ , CY has widest basin of attractor at  $u_0 = 0.20 \sim 0.35$  and LM has the widest has the widest basin of attractor at  $u_0 = 0.40 \sim 0.50$ , which are identical with Fig. 5.

#### 4. Discussion

We have examined 3D aggregation patterns in the volume-filling KS model. Apart from lamellar, cylinder, and sphere patterns which are simple generalization of two-dimensional patterns, we have obtained new patterns called P-surfaces and perforated lamellar patterns. These patterns are characteristic in three dimensions.

When considering the 3D self-organized patterns in the related systems, for example 3D phase separation and pattern formation by Cahn-Hilliard equation, many researchers studied the numerical algorithm, physical index and so on (Badalassi *et al.*, 2003). They found that a surface domain with some curvatures would be the solutions in addition to lamellar, cylinder and sphere. In this paper, we have clearly shown that the ones of such surface are P surfaces and perforated lamellar in the 3D Keller-Segel models.

Finally, Haessler *et al.* (2011) have already addressed the 3D characteristic problem relating to chemotactic movement generated ligand gradients, which provides a general example of quantitative chemotaxis defined chemokine gradients in three dimensions. The 3D aggregation patterns in this paper will serve for considering experimental set up for the 3D chemotactic behaviors and their 3D analysis.

**Acknowledgments.** This work was performed in part under the Cooperative Research Program of Institute for Frontier Medical Sciences, Kyoto University, Japan.

#### References

- Badalassi, V. E., Ceniceros, H. D. and Banerjee, S. (2003) Computation of multiphase systems with phase field models, *J. Comp. Phys.*, **190**, 371–397.
- Chavanis, P. H. (2003) Generalized thermodynamics and Fokker-Planck equations: Application to stellar dynamics and two-dimensional turbulence, *Phys. Rev. E*, **68**, 036108.
- Dolak, Y. and Hillen, T. (2003) Cattaneo models for chemotaxis, numerical solution and pattern formation, *J. Math. Biol.*, **46**, 153–170.
- Haessler, U., Pisano, M., Wu, M. and Swartz, M. A. (2011) Dendritic cell chemotaxis in 3D under defined chemokine gradients reveals differential response to ligands CCL21 and CCL19, *Proc. Nat. Acad. Sci. USA*, **108**, 5615–5619.

- Hillen, T. and Painter, K. J. (2001) Global existence for a parabolic chemotaxis model with prevention overcrowding, *Adv. Appl. Math.*, **26**, 280–301.
- Hillen, T. and Painter, K. J. (2009) A user's guide to PDE models for chemotaxis, *J. Math. Biol.*, **58**, 183–217.
- Horstmann, D. (2003) From 1970 until present: Keller-Segel model in chemotaxis and its consequences, *I. Jahre. DMV*, **105**, 103–165.
- Keller, E. F. and Segel, L. A. (1970) Initiation of slime mold aggregation viewed as an infinity, *J. Theor. Biol.*, **26**, 399–415.
- Luzzati, V. and Spegt, P. A. (1967) *Nature*, **215**, 701, London.
- Murray, J. D. (1993) *Mathematical Biology*, 2nd ed., Springer.
- Nagai, T. (1995) Blow-up of radially symmetric solutions to a chemotaxis system, *Adv. Math. Sci. Appl.*, **5**, 581–601.
- Schwarz, H. A. (1890) *GesammelZe Mathematische Abhandlungen*, Bd. I., Springer, Berlin.